American Journal of Pathology, Vol. 140, No. 3, March 1992

Canine G_{M1}-gangliosidosis

A Clinical, Morphologic, Histochemical, and Biochemical Comparison of Two Different Models

J. Alroy,* U. Orgad,*† R. DeGasperi,‡ R. Richard,*‡ C. D. Warren,‡ K. Knowles,‖ J. G. Thalhammer,‖ and S. S. Raghavan¶

From the Department of Pathology, Tufts University Schools of Medicine and Veterinary Medicine, Boston, Massachusetts; the Department of Pathology,† Koret School of Veterinary Medicine, Hebrew University of Jerusalem, Rehovot, Israel; the Laboratory for Carbohydrate Research,‡ Massachusetts General Hospital, Boston, Massachusetts; the Department of Medicine,‖ Tufts University School of Veterinary Medicine, Grafton, Massachusetts; and the Department of Biochemistry,¶ E. K. Shriver Center for Mental Retardation, Waltham, Massachusetts*

The clinical, morphologic, histochemical, and biochemical features of G_{M1}-gangliosidosis in two canine models, English Springer Spaniel (ESS) and Portuguese Water Dog (PWD), have been compared. The disease onset, its clinical course, and survival period of the affected dogs were similar in both models. Skeletal dysplasia was noted radiographically at 2 months of age, whereas at 4½ months of age there was progressive neurologic impairment. However, dwarfism and coarse facial features were seen only in ESS. Both models had similar deficiency in activity of lysosomal β-galactosidase, but possessed a normal protein activator for G_{M1}-β-galactosidase. Both models stored G_{M1}-ganglioside, asialo-G_{M1}, and oligosaccharides in brain. Furthermore, only the PWD stored glycoproteins containing polylactosaminoglycans in visceral organs, and neither model stored them in the brain. Morphologically, both models demonstrated similar storage material in multiple tissues and cell types. The ultrastructure of the storage material was cell-type specific and identical in both models. However, some differences in the lectin staining pattern were noted. Our clinical, biochemical, and histochemical findings indicate that PWD and ESS may represent two different mutations of the β-galactosidase gene. Moreover, the authors conclude that it is difficult, and inappropriate, to apply the human classification of G_{M1}-gangliosidosis (i.e., infantile, juvenile, and adult forms) to these canine models. (Am J Pathol 1992, 140:675–689)

GM1-gangliosidosis is a lysosomal storage disease caused by deficient activity of lysosomal acid β-galactosidase. This results in lysosomal accumulation of glycolipids and oligosaccharides with a nonreducing terminal β-galactosidic linkage in multiple tissues and various cell types, as well as the abnormal excretion of various compounds in urine.[1,2] In humans, this disorder is classified into three forms, infantile (type 1), juvenile (type 2), and adult (type 3), on the basis of age at onset of symptoms, temporal evolution, clinical and pathologic manifestations,[2] the excretion of urinary oligosaccharides,[3] and quantities of cholesterol, phospholipids, cerebrosides, and sulphatides in brain.[4] G_{M1}-gangliosidosis has been identified and studied in cats,[5,6] cattle,[7] dogs,[8–12] and sheep.[13–16] In cats, cattle, dogs, and sheep[5–9,11–16] the affected animals do not have skeletal involvement and thus they are clinically similar to the juvenile (type 2) form of the disease in humans.

In this study, we have compared the clinical, biochemical, and morphologic manifestations of G_{M1}-gangliosidosis in the English Springer Spaniel (ESS)[10] and Portuguese Water dog (PWD).[11–12] Unlike other animal models for G_{M1}-gangliosidosis, these models are characterized by skeletal lesions.[17] Our work demonstrated that the two models have similar age of onset, organ involvement, bone dysplasia, residual enzyme activity, and lymphocyte vacuolations, but they differ in the visceral storage of glycoproteins containing polylactosaminoglycans,[18] as well as in the presence of coarse facial features, noted only in the ESS model.[10]

Supported by grant NS 21765 from the National Institute of Neurological and Communicative Disorders and Stroke grant HD 21087 from the National Institute of Child Health and Human Development, and by Summer Stipend from the March of Dimes Birth Defects Foundation.

Accepted for publication October 22, 1991.

Address reprint requests to Dr. Joseph Alroy, Department of Pathology, Tufts University Schools of Medicine and Veterinary Medicine, 136 Harrison Avenue, Boston, MA 02111.

Materials and Methods

We studied eleven affected PWD dogs, three affected ESS dogs, and corresponding age and sex-matched controls. Three of eighteen affected puppies were diagnosed at birth by using β-galactosidase assay, analysis for oligosaccharides characteristic of G_{M1}-gangliosidosis, and electron microscopic examination of their placentas, as was previously reported in cats with α-mannosidosis.[19] Another three affected PWD dogs from a litter of ten were diagnosed by determination of β-galactosidase activity in their umbilical cord (this determination was done by Dr. J.S. O'Brien (University of California, San Diego). In both cases their clinically normal siblings served as controls. Their diagnosis and the diagnosis of eight other dogs was confirmed after 7 weeks by the assay of β-galactosidase activity in white blood cells. The determinations for white blood cell pellets and placentas were done in duplicate using synthetic fluorogenic 4-methylumbelliferyl β-galactoside as substrate. The values were compared with those obtained from their siblings, 29 unrelated ESS dogs, 786 unrelated PWD, and in some cases by additional examination of an air-dried blood smear, stained with Wright Giemsa, and by electron microscopy evaluation of buffy coats. The animals underwent monthly physical and neurologic examinations, which included recording of visual-evoked potentials (VEPs). The procedure of recording the VEPs has been described previously in cats with α-mannosidosis.[20] The dogs had radiographic examinations at 2 months of age and thereafter every 3 months. At 9 months, the skulls of affected ESS and PWD dogs, and one control ESS, were evaluated with nuclear magnetic imaging (MRI).[21] Urine specimens from both affected and control ESS and PWD were collected for oligosaccharide analysis, and urine from four dogs was taken to determine the presence and activity of G_{M1}-activator protein, which stimulates the degradation of G_{M1} to G_{M2}, and processed as previously described[22] (this assay was done by Dr. Y-T Li, Tulane University). Affected dogs and age-matched controls were euthanatized at 2, 3, 4, 5, 7, 8, and 9 months of age with intravenous injection of sodium pentobarbital, and necropsied (4 dogs were necropsied at Colorado State University). Samples from each dog were taken for light and electron microscopy and for biochemical studies. Tissue and body fluid specimens for biochemical studies were immediately removed and stored frozen at −70°C until used.

Electron and Light Microscopy

For electron microscopic studies the samples were fixed in Trump's fixative in cacodylate buffer, pH 7.2; postfixed in 1% osmium tetroxide in 0.1 M cacodylate buffer, pH 7.4; dehydrated through graded ethanol solutions, and embedded in Embed-812 epoxy resin. For light microscopy 1-μm thick sections were stained with toluidine blue (TB). For electron microscopy, 50–70 nm thin sections were cut and stained with uranyl acetate and lead citrate. Unfixed brain tissues were obtained for frozen sections. They were embedded in OCT compound (Miles Inc. Elkhart, IN) and stained with periodic acid-Schiff (PAS), Sudan black, and biotinylated lectins. The remainder of the tissue was fixed in 10% buffered formalin, embedded in paraffin, processed for light microscopy, stained with hematoxylin and eosin (H&E), and 11 different lectins. In addition, the brain sections were stained with luxol fast blue (LFB), whereas the bones were stained with safranin-O.

Lectin Histochemistry

Table 1 lists the lectins used in this study, their acronyms, the lectin concentrations used, their major sugar specificity, and the corresponding sugars used to inhibit their tissue binding. Detailed protocols for the lectin staining on paraffin and frozen sections and on the control tissue have been reported earlier.[23,24] Lectin cytochemistry at the ultrastructural level was done on a skin biopsy of an affected PWD dog. The tissue was embedded at low temperature in Lowicryl K4M and stained only with *Ricinus communis* agglutinin-I (RCA-I) conjugated to gold particles, which were 15 nm in diameter.[25]

Glycolipid Analysis

Brain tissue (0.52 g) from two control and two affected PWD was homogenized in 5 ml water and extracted overnight with 100 ml of chloroform:methanol (C:M, 2:1). The extract was filtered through a sintered glass funnel and residue reextracted with 50 ml of the same solvent. The combined filtrate was dried in a flash evaporator and the residue was taken up in 10 ml of C:M (2:1) and washed.[26] Gangliosides and minor amounts of neutral glycosphingolipids with long oligosaccharide chains, such as asialo-G_{M1}, present in the aqueous upper phase, were purified by chromatography on a BondElut C18 cartridge containing 500 mg of absorbent.[27] The bulk of the neutral glycosphingolipids including asislo-G_{M1} were present in the lower (i.e., organic) phase. Total gangliosides were quantitated by sialic acid determination,[28] using the modified procedure for the elimination of interference by pH-dependent extraction of the chromogen.[29] Individual gangliosides were separated by high performance thin layer chromatography (HPTLC).[30] Minor amounts of neutral glycosphingolipids with long oligosaccharide side chains, such as asialo G_{M1}, were separated from the gangliosides by chromatography on

Table 1. *Lectins Used for Identifying Carbohydrate Residues*

Lectin origin	Common name	Acronym	Concentration (μg/ml)	Major sugar specification*	Binding inhibitor
Arachis hypogea	Peanut	PNA	20	Gal-β-(1-3)-GalNAc	Lactose
Concanavalia ensiformis	Jack bean	Con A	10	α-D-Glc, α-D-Man	α-D-methyl-Man
Datura stramonium	Jimsonweed	DSA	10	[β-D-Gal-(1 → 4)-β-D-GlcNAc-(1 → 3)]$_n$	(β-D-GlcNAc)$_{2-3}$
Dolichos biflorus	Horse gram	DBA	10	α-D-GalNAc	α-D-GalNAc
Glycine max	Soybean	SBA	10	α-D-GalNAc, α-D-Gal	α-D-GalNAc
Griffonia simplicifolia	Bandeirea	GS-I	50	α-D-Gal	Lactose
Lens culinars	Common lentil	LCA	10	α-D-Glc, α-D-Man	α-D-methyl-Man
Ricinus communis	Castor bean	RCA-I	50	β-D-Gal	Lactose
Triticum vulgaris	Wheat germ	WGA	50	[β-(1 → 4)-D-GalNac]$_2$ NeuNAc	NeuNAc
	Succinyl-WGA	S-WGA	10	[β-(1 → 4)-D-GlcNAc]$_2$	β-D-GlcNAc
Ulex europaeus	Gorse	UEA-I	10	α-L-fucose	α-L-fucose

* Gal, galactose; GalNAc, N-acetylgalactosamine; Glc, glucose; Man, mannose; GlcNAc, N-acetylglucosamine; NeuNAc, N-acetylneuraminic acid (sialic acid).

DEAE-sephadex packed to a height of 7 cm in Pasteur pipette.[30]

Total lipids from the washed lower phase were fractionated by chromatography on 1 g silicic acid packed in chloroform to a height of 6 to 8 cm. After applying the sample in chloroform, nonpolar lipids were eluted with 40 ml of chloroform. Glycosphingolipids were eluted with 60 ml of acetone:methanol (9:1) after which phospholipids were obtained by elution with 60 ml of methanol. The glycosphingolipid fraction was subjected to alkaline hydrolysis to remove any ester lipid contaminant and then separated into individual components as cerebroside, sulfatide and asialo G_{M1}, by thin-layer chromatography (TLC). For quantitation, cerebroside and asialo-G_{M1} were separated from sulfatide by chromatography on DEAE-sephadex as outlined for the gangliosides. The cerebroside-asialo G_{M1} fraction was further purified by silicic acid chromatography using acetone as the eluant so that asialo G_{M1} would be retained on the column to be eluted later with methanol. Cerebroside and sulfatide were quantitated by the orcinol sulfuric acid reaction.[29]

Immunoblot analysis for G_{M1} with cholera toxin, and for asialo G_{M1} with a specific monoclonal antibody, was performed as previously described.[31]

Oligosaccharide Analysis

Oligosaccharides were isolated from urine (1 ml) by gel-filtration and deionization as previously described,[32] and analyzed by high pressure liquid chromatography (HPLC) on an Amino-Spherisorb column.[32,33] Oligosaccharides were identified by comparison of the chromatographic profile with that of a sample prepared from the liver of a dog with G_{M1} gangliosidosis,[34] and quantified by the chromatography, under identical conditions, of a sample of di-*N*-acetylchitobiose, followed by a calculation based on the sum of the integrated areas of four oligosaccharide peaks, compared with the area of the di-*N*-acetylchitobiose peak (detection by UV absorption at 195 nm). The resulting concentrations (nmol/μl) were normalized for creatinine, determined in (mg/μl) on a portion of the same sample of urine as that employed for oligosaccharide analysis. Oligosaccharides were extracted from tissues as described previously for cats with α-mannosidosis[35] and the extracts were analyzed by HPLC as described earlier for urine. A sample of serum from affected PWD (1.5 ml), and the same volume of control dog serum, were lyophilized and extracted with ethanol:H_2O (1:1, 5 ml) by repeated vortex mixing. The supernatant was evaporated to dryness, and the residue was dissolved in H_2O (1 ml) and passed through coupled columns (0.5 × 2.5 cm) of AG 1 × 2 (formate) and AG 50 × 2) (H^+) ion-exchange resins (BioRad Laboratories, Richmond, CA). Subsequent treatment and analysis were performed as described earlier for urine.

Results

Biochemical and Morphologic Findings in Placentae, Amniotic Fluids, and Umbilical Cords

Lysosomal β-galactosidase activity of placentae from three affected puppies ranged from 24 to 92 units (nmoles of 4-methylumbelliferone released/mg protein/hr), with 68 ± 38 (mean ± standard deviation) which was less than 10% of control (1,110 ± 270), whereas the enzyme activity of presumptive heterozygotes had a mean of 290 ± 122, which is less than 50% of control. The activity of lysosomal β-galactosidase in umbilical cords of three affected puppies varied from 8 to 22 units, with a mean of 15 ± 4; the activity in five presumptive carriers was 165 ± 45, whereas in two presumptive normals the mean was 281 ± 5.

Oligosaccharides extracted from placentae and from amniotic fluids analyzed by normal phase HPLC showed large peaks with the characteristic pattern for G_{M1}-gangliosidosis only in affected puppies,[18] but not in presumptive carriers or normal puppies.

Canine placenta is of the zonary endotheliochorial type.[36] We were unable to distinguish between placentae of affected and normal puppies on light microscopy of paraffin sections stained with H&E, with lectins, or in 1-μm epoxy resin sections stained with toluidine blue. Ultrastructural examinations of placentae from affected puppies revealed numerous cytoplasmic vacuoles (i.e., secondary lysosomes) in fetal capillary endothelium (Figures 1, 2) and in mesenchymal cells. The lysosomes contained both membrane fragments as well as fibrillar material. Occasionally, extracellular lamellated membrane structures were observed in close proximity to the plasmalemma and lysosomes (Figure 2).

Clinical Observations

At 4½ months of age puppies of both models developed progressive ataxia, tremor, dysmetria, reduced menace responses, decreased cranial nerve responses, and nystagmus. VEP at 5 months of age revealed asymmetry (Figure 3). The affected ESS puppies were proportionately dwarfed, with frontal bossing and hypertelorism (Figure 4). Radiographs of the vertebral column obtained at 2 months showed irregular intervertebral disk spaces in affected ESS and PWD puppies. The severity of the skeletal lesions increased with age, and they were most prominent at the lumbar spine (Figure 5). Examinations of blood smears from both mutants revealed large numbers of vacuolated lymphocytes. Ultrastructural studies of the buffy coat exhibited vacuolated lymphocytes (Figure 6) and the presence of lamellated membrane structures in eosinophils. MRI of brain affected PWD and ESS from 9-month-old male, compared with brain of a normal ESS, showed enlarged gray matter and decreased cerebral and cerebellar white matter.[21]

Necropsy Findings

The most prominent gross changes were noted in the vertebral column and in the brain. A longitudinal section through the vertebral column revealed abnormal wid-

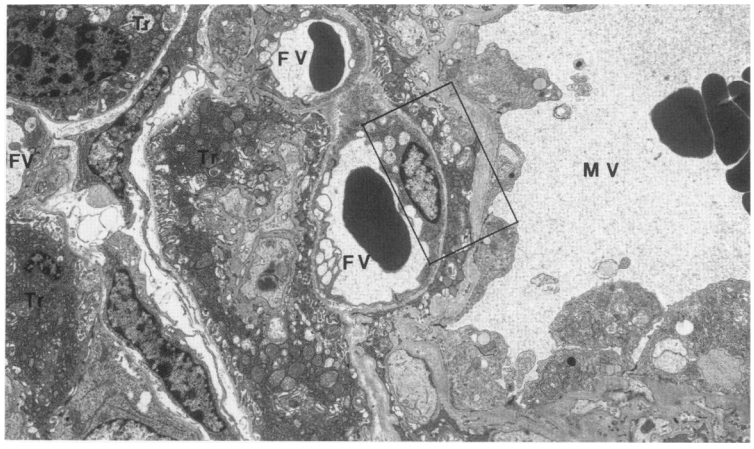

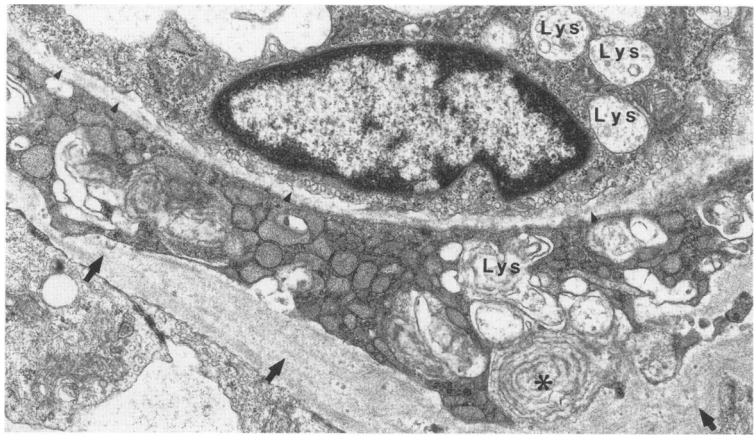

Figure 1. *Electron micrograph of placenta from an affected puppy, in which the activity of lysosomal β-galactosidase was 87 nmoles/mg protein/hr, illustrating trophoblasts (Tr), maternal vessel (MV), fetal vessels (FV) and fetal fibroblasts. The maternal endothelium is thick, whereas the fetal endothelium is thin. The fetal endothelium is vacuolated, ×4000.*
Figure 2. *Close-up of fetal endothelium and fibroblast, illustrating secondary lysosomes (Lys) laden with membrane fragments and fibrillar material. The extracellular space contained lamellated membrane structures (asterisk) adjacent to lysosomes. The fetal endothelium is surrounded by a single layer of basal lamina (arrowheads), whereas the maternal endothelium is surrounded by several layers of basal laminae (arrows), ×18,250.*

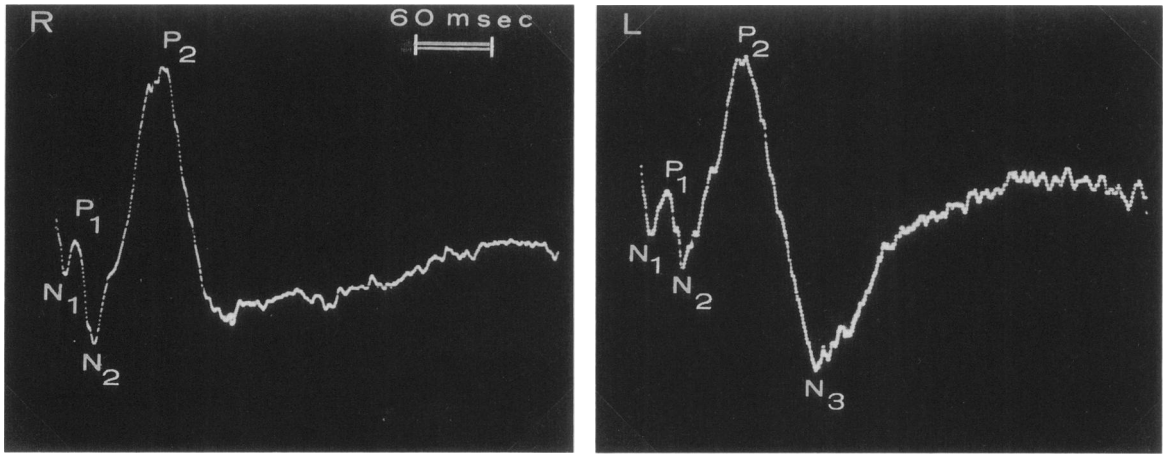

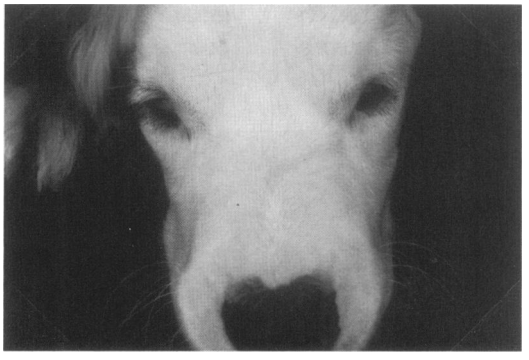

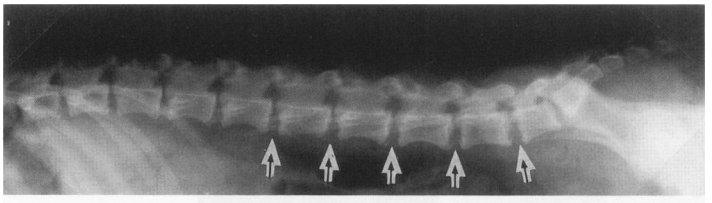

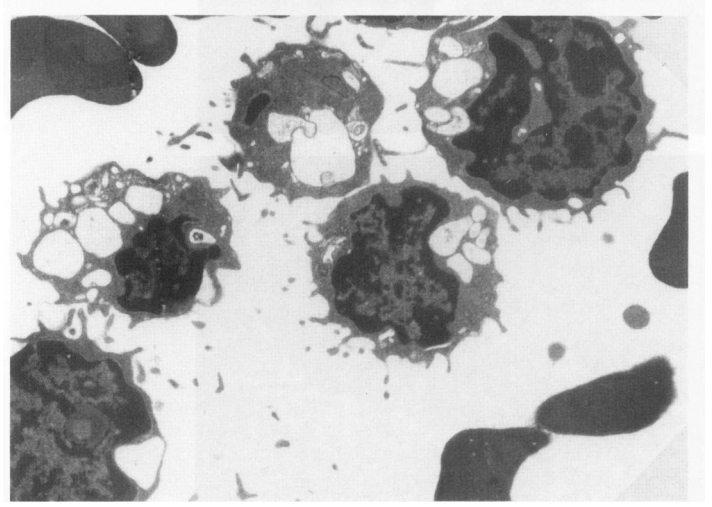

Figure 3. *Visual evoked potential recorded from a 5½-month-old affected Portuguese water dog. It represents the average signal of 130 recordings. Traces of right (R) and left (L) eyes demonstrate asymmetry in the positive (P) but not in the negative (N) components. Note the small differences in the length of the peaks between the R and L eyes.*

Figure 4. *Frontal view of the head of an 8-month-old English Springer Spaniel, affected with G_{M1}-gangliosidosis. The interorbital distance is abnormally increased (i.e., hypertelorism).*

Figure 5. *A lateral projection of a 5½-month affected female PWD's lumbar spine. The intervertebral discs (arrows) are deformed, irregular, and abnormally wide.*

Figure 6. *Electron micrograph of circulating lymphocytes from affected PWD. Both types of lymphocytes, those with convoluted and those with nonconvoluted nuclei, contain numerous vacuoles, ×8100.*

ened intervertebral disk spaces and abnormal ossification of vertebral physes. Coronal sections through the brain of affected puppies, aged 2 to 9 months, demonstrated progressive increased amounts of gray matter and small amounts of white matter. At 9 months of age, the wet weight ratio of white to gray matter from the frontal lobe was 1.1 in normal ESS puppy, 0.122 in affected ESS, and 0.29 in affected PWD, respectively.

Histological, Histochemical, and Ultrastructural Findings

Histopathologic examinations of brain, spinal cord, retina and peripheral ganglion, stained with H&E, revealed enlarged neurons, with pale foamy cytoplasm. The neuronal size, and the staining intensity of their cytoplasm, varied according to the age of the dog, as well as the site of the neurons. LFB-stained paraffin sections revealed light blue cytoplasmic inclusions. These inclusions stained dark blue with TB on resin-embedded brain tissue (Figure 7). The central cerebral and cerebellar folia exhibited astrocytosis, microgliosis, only a few macrophages, and scant myelin. The poor myelination could be best demonstrated with LFB and TB-stained sections (Figures 7, 8). The degree of brain myelination varied according to the location. In 9-month-old affected ESS and PWD, the corpus callosum and fornix stained intensely (but less so than a corresponding age and sex-matched ESS sibling), whereas the corona radiata stained lightly. The cytoplasm of neurons in unfixed, frozen sections, stained positively with PAS and Sudan black.

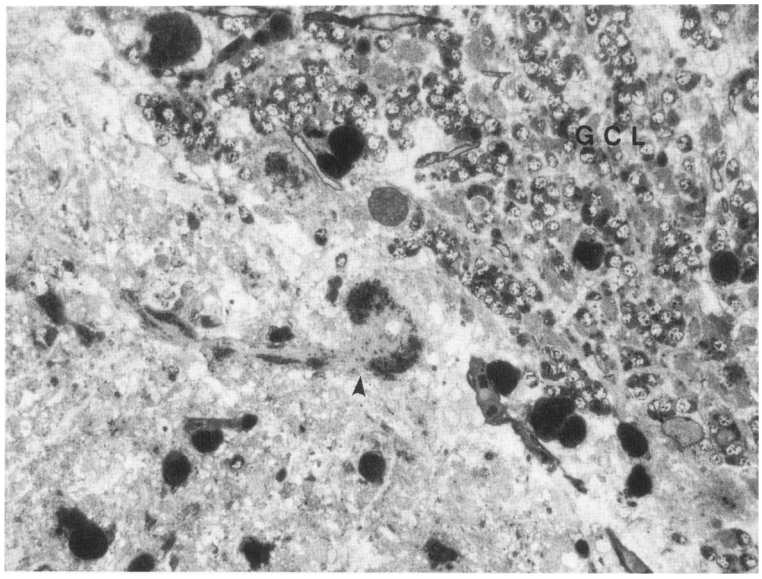

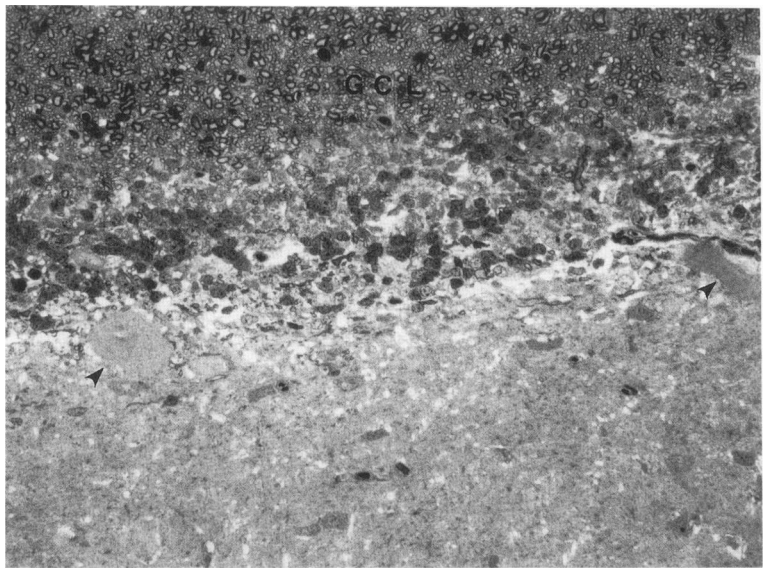

Figure 7. *One-μm thick section of cerebellum from an affected 9-month-old PWD. Purkinje cells (arrowhead), neurites, and astrocytes are enlarged and contain lipid-rich vesicles. Note the absence of myelin in the granular cell layer (GCL). Toluidine blue, ×272.*

Figure 8. *One-μm thick section of cerebellum from a control 10-month old PWD. The Purkinje cells, their neurites (arrowheads), and astrocytes, appear normal and the granular cell layer (GCL) is rich with myelin. Toluidine blue, ×272.*

A section of the vertebral column, stained with H&E and with safranin-O, revealed retarded ossification and cartilage necrosis at the ventral aspect of the lumbar spine physes. On light microscopy, infiltration of enlarged macrophages was noted in thymus, lymph nodes, Peyer's patches, and lung. Kupffer cells were enlarged and vacuolated, and many of the hepatocytes were vacuolated. Pancreatic islet and acinar cells, adrenal cortical, and medullary cells, renal proximal tubular cells, serous and mucinous cells of salivary glands and chondrocytes, all contained cytoplasmic vacuoles. Vacuolated keratocytes and ciliary epithelium were noted in TB-stained 1 μm sections of resin-embedded corneas and ciliary bodies.

Neurons from affected PWD and ESS stained only with RCA-I in fresh or formalin-fixed frozen sections, but did not stain in lipid-depleted frozen sections or paraffin sections, indicating neuronal storage of glycolipids with nonreducing β-galactosyl residues.[18] Also, neurons in paraffin sections of brains from affected PWD and ESS dogs stained with Con A and UEA-1. In addition, the neurons of affected ESS, but not PWD (Figure 9d), stained with *Dolichos biflorus* agglutinin (DBA), *Griffonia simplicifolia*-I (GS-I) (Figure 9 a,b,c) and soybean agglutinin. Furthermore, paraffin sections from affected cells in various sites, e.g., parenchymal organs and cartilage, stained intensely with RCA-I, whereas in normal animals the neurons either did not stain or the staining was weaker than in affected dogs.

Ultrastructural studies of both models demonstrated storage material in neurons, astrocytes, and endothelial cells (Figure 10), in different types of retinal cells, in corneal epithelium and keratocytes, in macrophages, in hepatocytes and Kupffer cells, in adrenal medulla cells, in chondrocytes, in glomerular podocytes, mesangial cells and endothelial cells (Figure 11), in renal tubular cells, in pancreatic ductal, acinar and in islet β-cells. Furthermore, storage material was noted in salivary ductal, se-

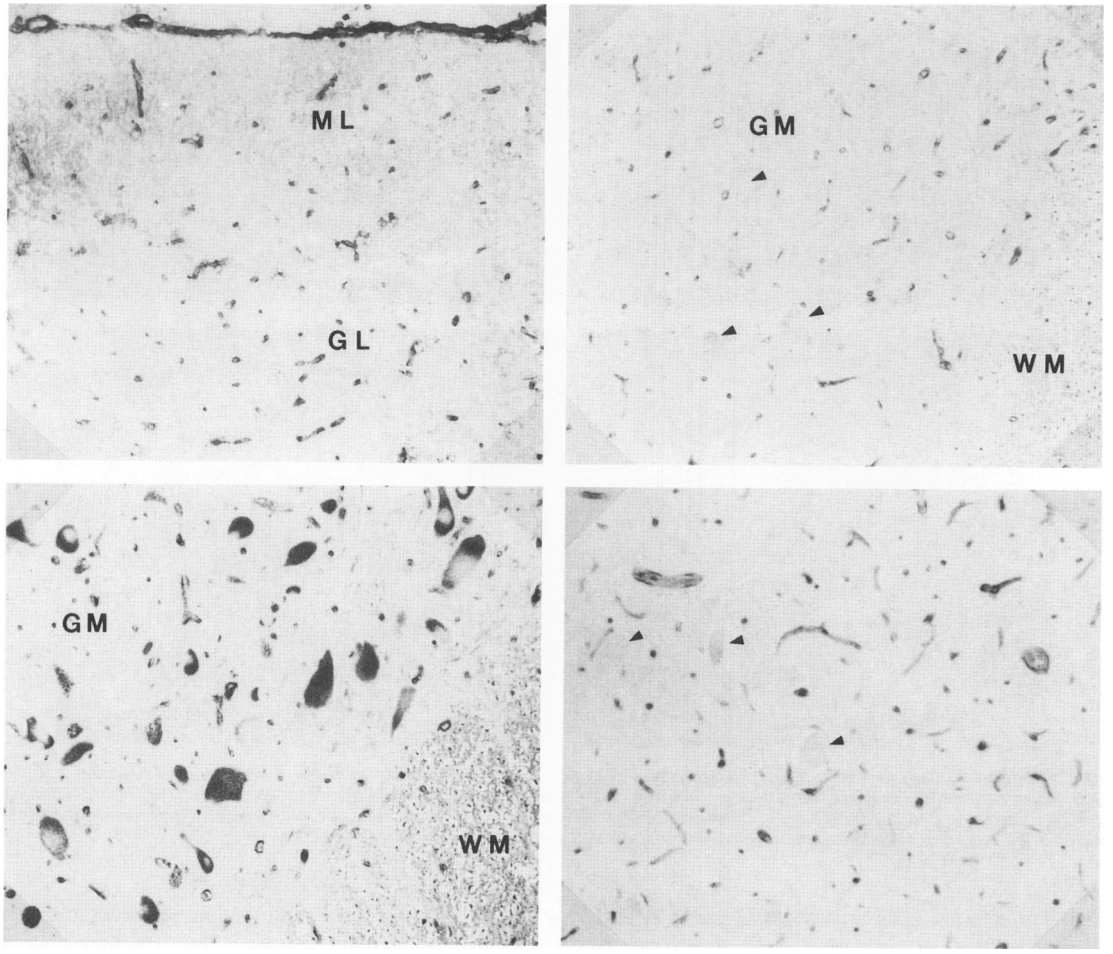

Figure 9. *Tissue sections of 9-month-old male dogs stained with* **Griffonia simplicifolia** *agglutinin-I.* **A:** *Frozen section through cerebellum of an affected ESS, only the vascular endothelium in the meninges, in the molecular layer (ML) and granular layer (GL), are stained. The neurons are unstained.* **B:** *Paraffin section of spinal cord from a normal control ESS, a litter mate of the affected ESS. Only the vascular endothelium in the gray matter (GM) and white matter (WM) are stained.* **C:** *Paraffin section of spinal cord from the same affected ESS as in* **(A).** *Both the vascular endothelium and the neuronal perikaryon are intensely stained.* **D:** *Paraffin section of spinal cord from an affected PWD. The vascular endothelium is positively stained, but the neurons (arrowheads) are unstained, ×81.*

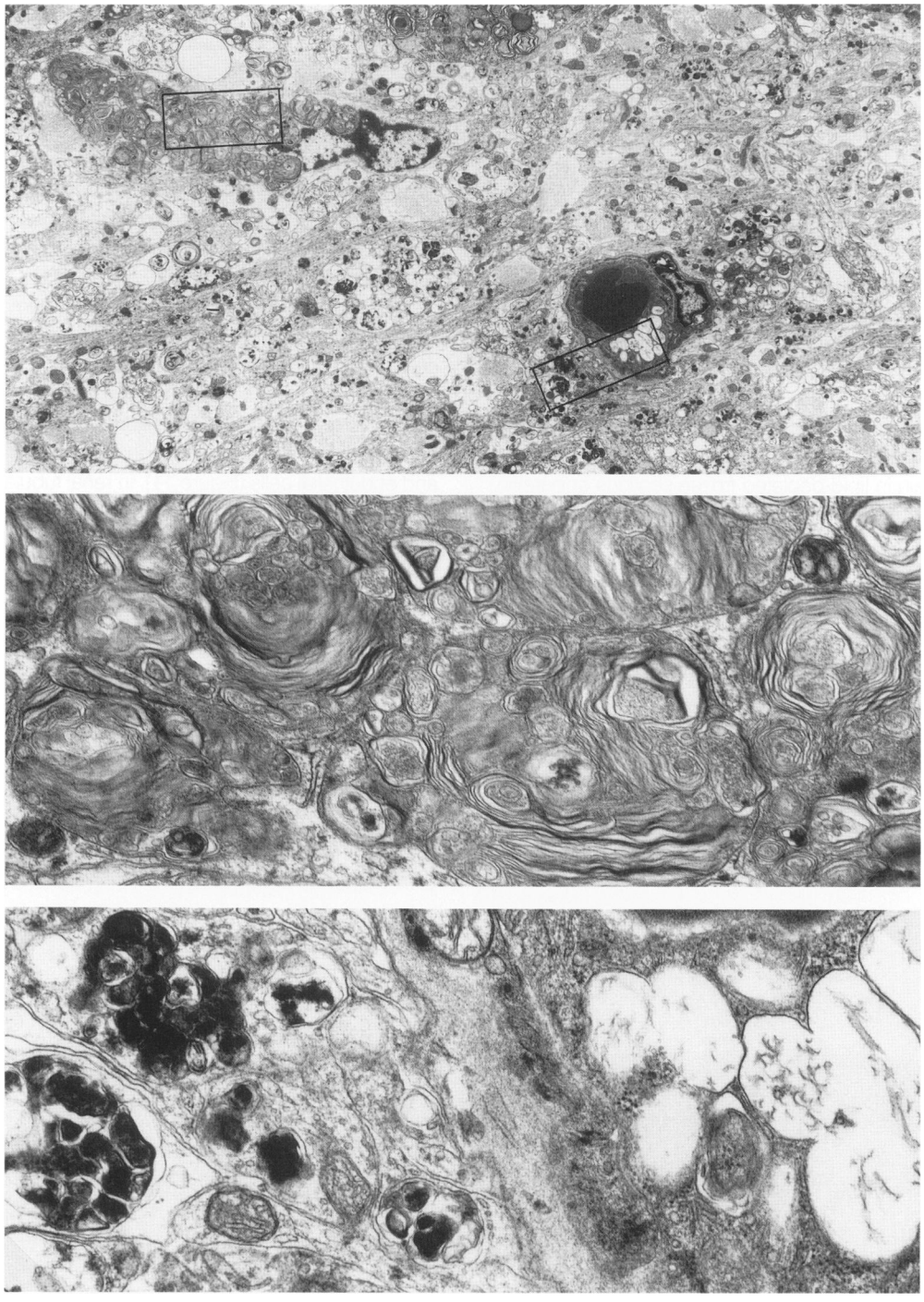

Figure 10. *Section through the brain of an affected dog, illustrating storage material in neurons, astrocytes, and vascular endothelium, ×3,800.* **A:** *Higher magnification of the neuron containing characteristic lamellated membrane structures. ×26,700. Inset* **B:** *Close view of the storage material in endothelial cell and adjacent axons. The former contains electron-lucent material and small membrane fragments, whereas the latter contains dense amorphous material mixed with membranous lamellae, ×26,700.*

rous and mucinous cells, in thyroid C cells, in aortic smooth muscle cells, and in dermal fibroblasts. The quantity and the morphology of the storage material varied according to the cell type. For example, in neurons (Figure 10A) and adrenal medulla cells, it appeared as lamellated membrane structures. However, the concentrations in the neurons were higher. The axons contained spheroids, a mixture of membrane structures and osmiophilic amorphous material that resembled lipofuscin (Figure 10B). Other cell types, such as endothelial cells

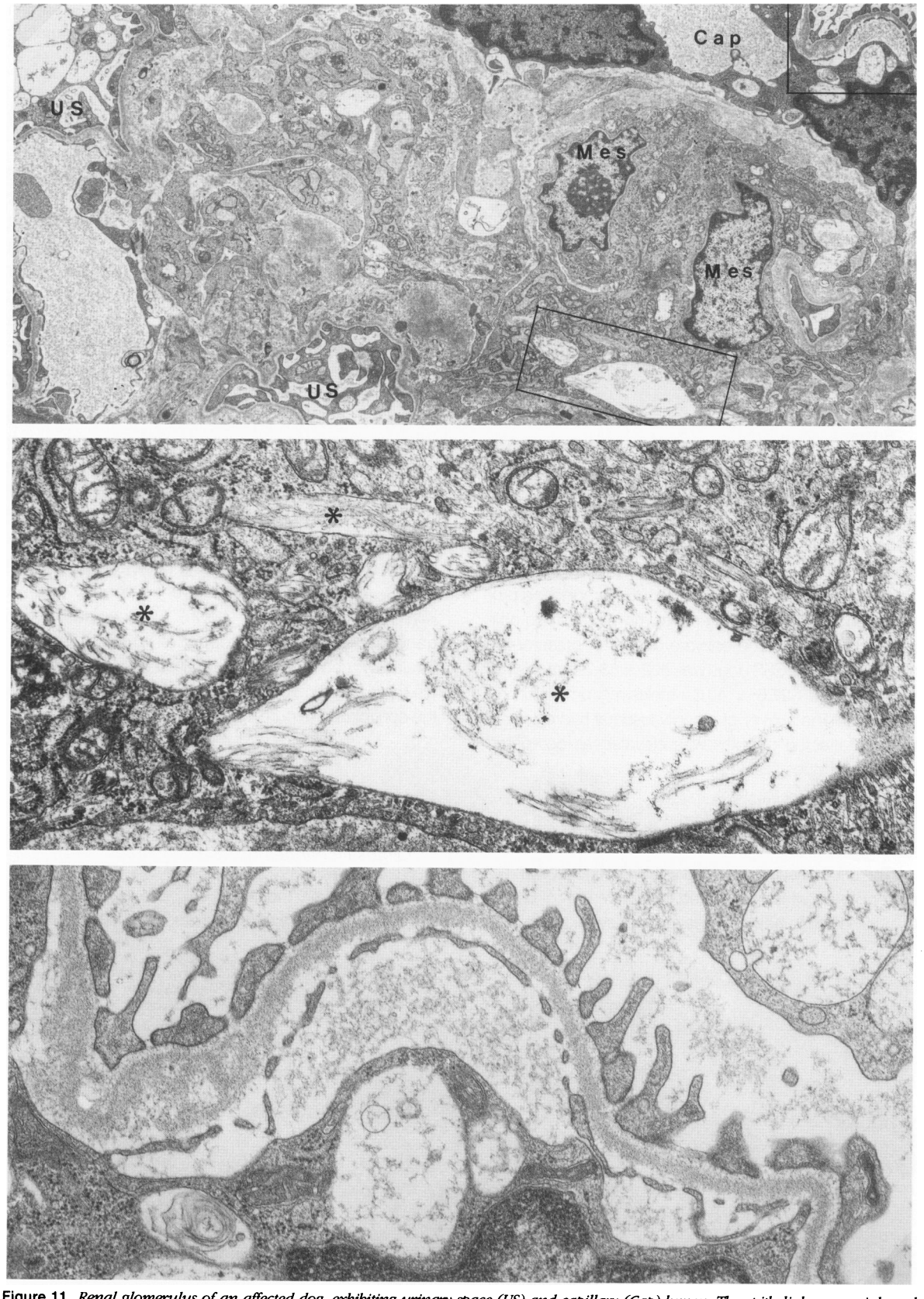

Figure 11. *Renal glomerulus of an affected dog, exhibiting urinary space (US) and capillary (Cap) lumen. The epithelial, mesangial, and endothelial cells are vacuolated, ×6,320. Inset* **A**: *The lysosomes in the mesangial cell contain twisted tubular structures (asterisks), ×26,700. Inset* **B**: *The lysosomes of both epithelial and endothelial cells contain fibrillo-granular material, ×26,700.*

(Figures 10B, 11B), or renal tubule cells, appeared empty or contained various amounts of fine fibrillar material occasionally accompanied by membrane fragments. In glomerular mesangial cells, the lysosomes contained twisted tubular structures (Figure 11A) that resembled the storage material seen in Gaucher's and Krabbe's disease.[37,38]

Electron microscopic examinations of low temperature Lowicryl K4M-embedded skin biopsies from an affected puppy, stained with RCA-1 conjugated to gold and revealed the presence of gold particles within cytoplasmic vacuoles (i.e., lysosomes) of dermal fibroblasts (Figure 12).

Biochemical Findings

Enzyme Analysis

Activity of lysosomal β-galactosidase, measured in white blood cells (WBC) from affected PWD puppies, was 19 ± 3.1 nmoles/mg protein/hr (mean ± standard deviation), and 17.75 ± 1.76 nmoles/mg protein/hr in affected ESS. The enzyme activity determined in WBC from obligate PWD carriers was 124.5 ± 35.7 nmoles/mg protein/hr and 67.75 ± 14.86 nmoles/mg protein/hr in obligate ESS carriers. The enzyme activity in presumptive normal PWD and ESS dogs was 302 ± 63.79 nmoles/mg protein/hr and 327.6 ± 43.3 nmoles/mg protein/hr, respectively. The activity of other lysosomal hydrolases in WBC of affected puppies was elevated as compared with normal dogs (Table 2).

Protein Activator Determination

The urine of affected ESS and PWD contained an activator protein which stimulated the conversion of G_{M1} to G_{M2} with human hepatic β-galactosidase. However, the dog activator protein did not crossreact with anti-human G_{M1}-activator protein (Dr. Y-T Li, personal communication).

Lipid Analysis

It is evident from Table 3 that total gangliosides, as assayed by the levels of lipid-bound N-acetylneuraminic acid (NANA), is markedly elevated in brain of affected dog as compared with control, whereas cerebroside content is severely diminished. This is indicative of either dysmyelination or demyelination. HPTLC of gangliosides (Figure 13) showed marked accumulation of G_{M1} in the diseased dog brain. This agrees with the severe deficiency of acid β-galactosidase in an affected dog brain, 2.1 (nmoles/mg protein/hr) compared with a brain of a control dog, 293 (nmoles/mg protein/hr). Accumulation of asialo G_{M1} could also be demonstrated in the diseased dog brain, see TLC (Figure 14) of the glycolipid fraction obtained by silicic acid chromatography of lipids from the lower phase of a Folch extraction.[18] This accumulation of G_{M1} and asialo G_{M1} was further confirmed by immunoblot analysis of TLC plates using cholera toxin to react with G_{M1} and a specific monoclonal antibody to react with asialo G_{M1} (data not shown). After separation from gangliosides by DEAE-sephadex chromatography, asialo G_{M1} could be clearly identified by TLC of the sample from an affected dog whereas it was hardly seen in the control dog (Figure 15).

Carbohydrate Analysis

Oligosaccharides Excreted in Urine

Urine from a 9-month-old G_{M1} ESS dog, a 9-month-old G_{M1} PWD dog, and an age- and sex-matched control

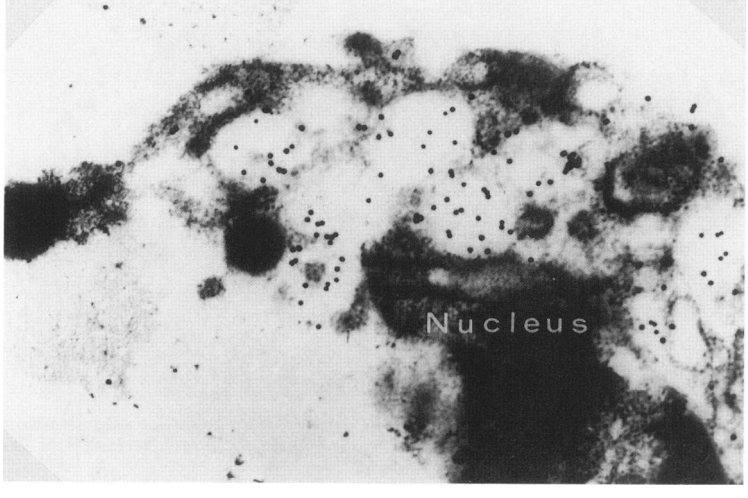

Figure 12. *Dermal fibroblast from an affected PWD, embedded in Lowicryl K4M at −35°C and stained with RCA-I. Note the presence of the black-gold particles in the vacuoles (i.e., secondary lysosomes) indicating the presence of compounds with nonreducing terminal β-galactosyl residues, ×31,000.*

Table 2. *Lysosomal Hydrolases in the Leukocytes from Normal Dogs and Dogs Affected with G_{M1}-gangliosidosis*

	Normal dogs	Affected dogs				
Enzyme	Mean SD (4)	PWD	PWD	PWD	PWD	ESS
β-Galactosidase	273.5 ± 9.2	4	24	19	19	17
α-Galactosidase	125.8 ± 11.4	134	—	—	—	206
α-Mannosidase	2033.8 ± 141.5	3820	—	2313	—	3850
β-Glucuronidase	296.3 ± 12.5	292	—	—	—	—
α-Fucosidase	113.3 ± 6.3	215	—	—	—	196
β-Hexosaminidase	3819.5 ± 439.9	4414	4256	2545	4829	5165
β-Glucosidase	88.5 ± 14.6	167	—	—	—	—

Activities are expressed as nmol of 4-methylumbelliferone (4-MU) liberated/mg protein/hr from the corresponding 4-MU-glycoside substrate.

ESS dog, was subjected to gel-filtration, deionization, and analysis by HPLC. Oligosaccharides, originating from the incomplete breakdown of *N*-linked glycans as a result of β-galactosidase deficiency, were present in the urine of both affected dogs (Figure 16 A, B)), but not in the control. The chromatographic profile was essentially the same for both dogs, and similar to that observed previously for an affected ESS.[10] The concentration of excreted oligosaccharides was 13.7 pmol/mg creatinine in the ESS dog and 9 pmol/mg creatinine in an age- and sex-matched PWD dog. Oligosaccharides with a chromatographic profile typical for G_{M1}-gangliosidosis were not observed in serum of an affected PWD dog (Figure 16C).

Oligosaccharides in Tissues of PWD

Oligosaccharides were analyzed by HPLC and were detected in adrenal, cardiac muscle, cerebellum, cerebrum, kidney, liver, lung, lymph node, pancreas, sciatic nerve, skeletal muscle, spinal cord, and spleen. The chromatographic profiles showed individual variations between tissues, but were always characteristic for G_{M1}-gangliosidosis.[10,18] Approximate quantitations based on the probable structures for the major oligosaccharides showed that kidney, liver, and pancreas contained the highest concentrations of oligosaccharides.

Discussion

These two canine models of G_{M1}-gangliosidosis share numerous clinical, morphologic, and biochemical features, but some significant differences were noted that may indicate that the affected dogs express different mutations. The levels of activity of lysosomal β-galactosidase, measured in WBC from affected PWD and ESS and assayed with an artificial substrate, were similar. The urine of both dog models contained a protein activator that stimulates the conversion of G_{M1}-ganglioside to G_{M2}.[22] These findings indicate that in both models the abnormal storage of G_{M1}-gangliosides in neurons, and oligosaccharides in tissue, is due to deficient activity of lysosomal β-galactosidase, rather than the deficient activity of the protein activator as reported in some forms of Gaucher disease,[39] metachromatic leukodystrophy,[40] and G_{M2}-gangliosidosis.[41] Affected puppies from both models can be diagnosed at birth by determination of lysosomal β-galactosidase activity in placenta or umbilical cord, by the chromatographic profile and amount of stored oligosaccharides in placenta or amniotic fluid, and by ultrastructural examinations. In both models the clinical signs and symptoms, as well as the alterations of parameters observed in neurophysiologic recordings, increased in severity with age, and this deterioration necessitated euthanasia when they reached 9 months of age. Morphologically, similar tissues and cell types were affected in both models. Cell types that are rich in G_{M1}-gangliosides, such as neurons,[42] or those of the adrenal medulla, contained enlarged secondary lysosomes that were laden with lamellated membrane structures. Other cell types including chondrocytes, endothelial cells, many endocrine and exocrine cells, fibroblasts, hepatocytes, Kupffer cells, lymphocytes, macrophages and various renal cell types contained enlarged secondary lysosomes that appeared empty or contained fine-fibrillar material. In addition, the lysosomes of the renal mesangial cells contained twisted tubular structures similar to those reported in affected cells from patients with Gaucher and Krabbe disease.[37,39] This differs from the storage seen in mesangial cells from cats with G_{M1}-gangliosidosis,[43] and from a 15-month-old child with the infantile form, in which the lysosomes appeared empty or contained fine-fibrillar material (Alroy, unpublished observations). These differences might indicate that canine

Table 3. *Glycosphingolipid Composition of Brain of Normal and G_{M1}-affected PWDS*

	Cerebrosides	Sulfatides	Gangliosides (lipid bound NANA)
Control dog	14.13	1.60	0.821
Affected dog	3.13	1.06	5.170

Values are expressed as μmol/g wet tissue.

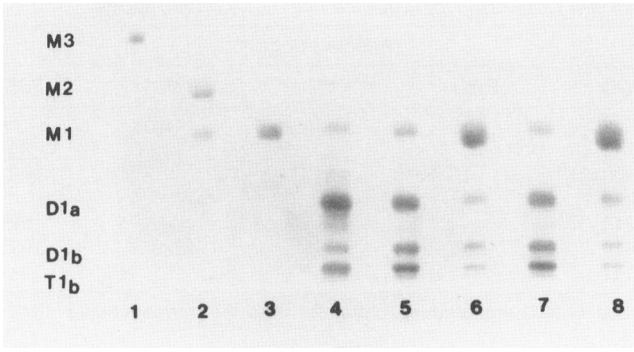

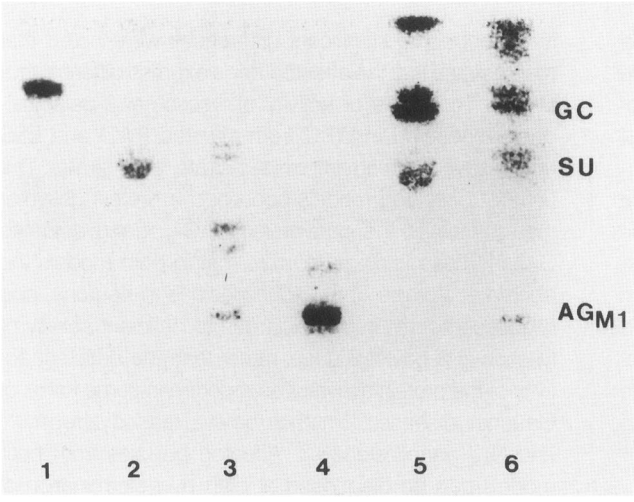

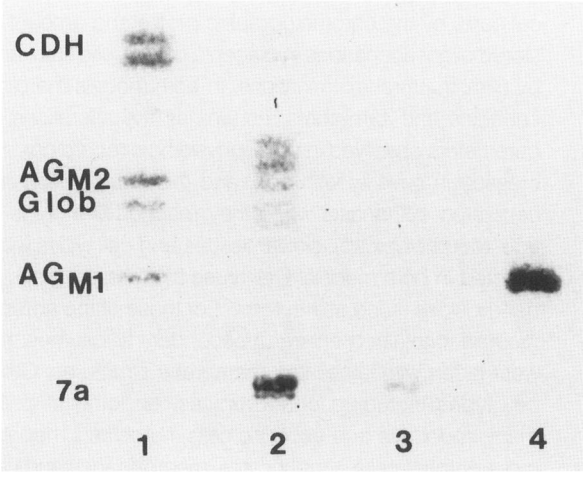

Figure 13. *Silicagel 60 HPTLC of brain gangliosides. Approximately four nmoles of lipid bound N-acetyl neuraminic acid from control and affected dog brain gangliosides were spotted. The plate was developed with a solvent system of chloroform:methanol:0.25% calcium chloride, 55:45:10, and spots were visualized by spraying with resorcinol. 1 = Std G_{M3}; 2 = Std G_{M2}; 3 = Std G_{M1}; 4 = Std brain gangliosides; 5 and 7 = control PWDs; 6 and 8 affected PWDs.*

Figure 14. *Silicagel 60 HPTLC of neutral glycosphingolipids of brain obtained from the lower phase of Folch extract. Five microliter of sample from 1 ml solution in C:M (2:1) was spotted on the plate. 1 = Std. Galactosylceramide (GC); 2 = Std. Sulfatide (SU); 3 = Std. mixture of lactosylceramide, asialo G_{M2} (AG_{M2}), globoside and AG_{M1}; 4 = Std. AG_{M1}; 5 = control PWD; 6 = affected PWD. The plates were developed with the solvent system of chloroform:methanol:water (C:M:W:, 60:35:8) and spots visualized by spraying with orcinol.*

Figure 15. *Silicagel 60 HPTLC of neutral glycosphingolipids of brain obtained after DEAE-sephadex chromatography of the upper phase of Folch extract. The small amounts of neutral glycosphingolipids recovered in this fraction were dissolved in 100 μl of C:M (2:1) and 10 μl aliquot was spotted. The plate was developed and spots were visualized as in Figure 14. 1 = Std. mixture of ceramide dihexoside/Lactosylceramide (CDH/Laccer), AG_{M2}, globoside and AG_{M1}; 2 = 7a glycolipid (stage-specific embryonic antigens) standard (47) obtained from Dr. McCluer at Shriver center; 3 = control PWD; 4 = affected PWD.*

mesangial cells catabolize different substrates from human or feline. Ultrastructural cytochemistry of dermal fibroblasts showed the binding of RCA-I-conjugated gold in lysosomes, indicating storage of nonlipid compounds (i.e., oligosaccharide) with terminal nonreducing β-galactosyl residues. Unlike previously reported models for G_{M1}-gangliosidosis,[5–8,14] both models displayed skeletal lesions that were observed radiographically, macroscopically, and microscopically. Skull lesions were noted in affected ESS but not in PWD.

Both ESS and PWD dogs excreted urinary oligosaccharides with a chromatographic profile typical of G_{M1}-gangliosidosis. That the profiles were similar does not necessarily imply that the oligosaccharide storage resulted from the same mutation in the β-galactosidase gene because it is well known that diverse genetic de-

Figure 16. *High-pressure liquid chromatograph of oligosaccharides extracted from urine and serum of dogs with G_{M1}-gangliosidosis.* **A**: *PWD urine.* **B**: *ESS urine.* **C**: *PWD serum. Extraction and sample preparation were performed as described in methods. The amount of sample injected corresponds to 0.042 ml urine* **(A)**, *0.1 ml urine* **(B)**, *and 0.3 ml serum* **(C)**. *Chromatography was on a Regis Hi-chrom reversible 5 μm Amino-Spherisorb column, with acetonitrile-water 7:3 at a flow rate of 2 ml/min, and detection by UV absorbance at 195 nm. The total elution time was 30 minutes for each run. The elution times of peaks 1 and 2 correspond to hexasaccharides, peak 3 to a heptasaccharide, and peak 4 to a nonasaccharide, respectively. The small peaks in* **C** *were also seen in the profile for control serum and therefore are not considered significant.*

fects can manifest themselves as similar functional defects. The urinary oligosaccharides could have originated from endogenous kidney glycoproteins or from the glomerular filtration of serum. Of all the tissues examined for oligosaccharide storage[18] the kidney had the highest concentration. However, even though typical G_{M1} oligosaccharides were not observed in a sample of affected PWD serum, it is still probable that the main bulk of oligosaccharides was derived from serum, as has been previously demonstrated for bovine α-mannosidosis.[44] Also a large disparity would be expected for the concentrations of oligosaccharides in urine and serum, as a result of glomerular filtration and tubular concentration. Furthermore, the levels of oligosaccharides in G_{M1} urine are similar to those observed in α-mannosidosis, which raises the possibility of enhanced renal clearance like that which occurs in α-mannosidosis.[45]

Previously, a major difference had been noted in the structures of glycopeptides isolated from the livers of ESS and PWD dogs with G_{M1}-gangliosidosis.[18] The glycopeptides from PWD liver and kidney were shown to contain polylactosaminoglycans, i.e., glycans containing lactosamine repeats, but the glycopeptides from ESS liver or kidney did not.[18] Polylactosaminoglycans had also been identified in brains and livers of human patients with infantile G_{M1},[46] but could not be demonstrated in the brains of affected ESS or PWD.

Classification of human G_{M1}-gangliosidosis into infantile (type 1), juvenile (type 2), and adult (type) forms was based on age of onset, and severity of clinical and pathologic manifestations. When more information became available concerning the various undegraded metabolites that are accumulated or excreted in these different forms, it became apparent that these distinctions may reflect different mutations. Therefore, the aforementioned classification may need to be reexamined. Similarly, caution should also be exercised in the classification of the various animal models of G_{M1}-gangliosidosis.

In conclusion, the similarities and the differences at the clinical, morphologic, and biochemical levels, between two canine mutant models for G_{M1}-gangliosidosis, were highlighted. The phenotypic differences in these two dog models for G_{M1}-gangliosidosis suggest that they may have originated from two distinct mutations in the β-galactosidase gene.

Acknowledgments

The authors thank Dr. Y-T Li, Tulane University, for the assay of protein activator; Dr. J. S. O'Brien, University of California, for the enzymatic assay of the umbilical cords; Dr. M. Natowicz, Shriver Center, for the determination of creatinine concentrations in urine; Dr. G. L. Cockerell, Colorado State University, for assistance with necropsying and collecting tissue samples; Mrs. P. Stuart-Volz and Mrs. J. Harding for their contributions; Mrs. V. Goyal for technical assistance; and Ms. C. Welch for assistance with the manuscript.

References

1. Landing BH, Silverman FN, Craig JM, Jacoby MD, Lahey ME, Chadwick DL: Familial neurovisceral lipidosis. An analysis of eight cases of a syndrome previously reported as "Hurler-variant," "Pseudo-Hurler disease," and "Tay-Sachs disease with visceral involvement." Am J Dis Child 1964, 108:503–522
2. O'Brien JS: β-Galactosidase deficiency (G_{M1} gangliosidosis, Galactosialidosis, and Morquio syndrome type B); Ganglioside sialidase deficiency (Mucolipidosis IV). The Metabolic Basis of Inherited Disease 6th edition. Edited by CR Scriver, AL Beaudet, WS Sly, D Valle. New York, McGraw-Hill, 1983, pp 1797–1806

3. Warner TG, Robertson AD, O'Brien JS: Diagnosis of G_{M1} gangliosidosis based on detection of urinary oligosaccharides with high performance liquid chromatography. Clin Chim Acta 1983, 127:313–326
4. Kasama T, Taketomi T: Abnormalities of cerebral lipids in G_{M1}-gangliosidosis, infantile, juvenile, and chronic type. Jpn J Exp Med 1986, 56:1–11
5. Baker HJ, Lindsey JR, McKhann GM, Farrel DF: Neuronal G_{M1} gangliosidosis in a Siamese cat with β-galactosidase deficiency. Science 1971, 147:838–839
6. Blakemore WF: G_{M1} gangliosidosis in a cat. J Comp Pathol 1972, 82:179–185
7. Donnelly WJC, Sheahan BJ: G_{M1}-gangliosidosis of Friesian calves. A review. Irish Vet J 1981, 35:45–55
8. Read DH, Harrington DD, Keenan TW, Hinoman EJ: Neuronal-visceral G_{M1} gangliosidosis in a dog with β-galactosidase deficiency. Science 1976, 194:442–445
9. Rodriguez M, O'Brien JS, Garrett RS, Powell HC: Canine G_{M1}-gangliosidosis. An ultrastructural and biochemical study. J Neuropathol Exp Neurol 1982, 41:618–629
10. Alroy J, Orgad U, Ucci AA, Schelling SH, Schunk KL, Warren CD, Raghavan S, Kolodny EH: Neurovisceral and skeletal G_{M1}-gangliosidosis in dogs with β-galactosidase deficiency. Science 1985, 229:470–472
11. Saunders GK, Wood PA, Myers RK, Shell LG, Carithers R: G_{M1} gangliosidosis in Portuguese water dogs: pathologic and biochemical findings. Vet Pathol 1988, 25:265–269
12. Shell LG, Potthoff A, Carithers R, Katherman A, Saunders GK, Wood PA, Giger U: Neuronal-visceral G_{M1} gangliosidosis in Portuguese water dogs. J Vet Intern Med 1989, 3:1–7
13. Ahern-Rindell AJ, Prieur DJ, Murnane RD, Ragavan SS, Daniel PF, McClure RH, Walkley SU, Parish SM: Inherited lysosomal storage disease associated with deficiencies of β-galactosidase and α-neuraminidase in sheep. Am J Med Genet 1988, 31:39–56
14. Murnane RD, Prieur DJ, Ahern-Rindell AJ, Parish SM, Collier: The lesions of an ovine lysosomal storage disease. Initial characterization. Am J Pathol 1989, 134:263–270
15. Murnane RD, Ahern-Rindell AJ, Prieur DJ: Lectin histochemistry of an ovine lysosomal storage disease with deficiencies of β-galactosidase and α-neuraminidase. Am J Pathol 1989, 135:623–630
16. Ahern-Rindell AJ, Murnane RD, Prieur DJ: Interspecies genetic complementation analysis of human and sheep fibroblasts with β-galactosidase deficiency. Somat Cell Genet 1989, 15:525–533
17. Orgad U, Schelling S, Alroy J, Rosenberg A, Schiller A: Skeletal lesions in lysosomal storage diseases. Lab Invest 1989, 60:68A
18. Alroy J, DeGasperi R, Warren CD: Application of lectin histochemistry and carbohydrate analysis to the characterization of lysosomal storage diseases. Carbohydr Res 1991, 213:229–250
19. Alroy J, Warren CD, Raghavan SS, Daniel PF, Schunk KL, Kolodny EH: Biochemical ultrastructural and histochemical studies of cat placentae deficient in α-mannosidase. Placenta 1987, 8:545–553
20. Alroy J, Bachrach A, Thalhammer JG, Panjwani N, Richard R, DeGasperi R, Warren CD, Albert DM, Raghavan SS: Clinical, neurophysiological, biochemical and morphological features of eyes in Persian cats mannosidosis. Virchows Arch B 1991, 60:173–180
21. Kaye ED, Adelman L, Alroy J, Raghavan SS, Runge V, Gelblum D, Thalhammer JG: Leukodystrophy in G_{M1} gangliosidosis. Ann Neurol 1989, 26:434A
22. Li YT, Muhiudeen IA, DeGasperi R, Hirabayashi Y, Li SC: Presence of activator proteins for the enzymic hydrolysis of G_{M1} and G_{M2} gangliosides in normal human urine. Am J Hum Genet 1983, 35:629–634
23. Alroy J, Ucci AA, Goyal V, Woods W: Lectin histochemistry of glycolipid storage diseases on frozen and paraffin-embedded tissue sections. J Histochem Cytochem 1986, 34:501–505
24. Alroy J, Goyal V, Warren CD: Lectin histochemistry of gangliosidosis. I. Neural tissue in four mammalian species. Acta Neuropathol 1988, 76:109–114
25. Roth J: Cytochemical localization of terminal N-acetyl-D-galactosamine residues in cellular compartments of intestinal goblet cells: Implications for the topology of O-glycosylation. J Cell Biol 1984, 98:399–406
26. Folch J, Lees M, Sloane-Stanley GH: A simple method for the isolation and purification of total lipids from animal tissues. J Biol Chem 1957, 226:497–509
27. Williams MA, McCluer RH: The use of Sep-PaK C18 cartridges during the isolation of gangliosides. J Neurochem 1980, 35:226–269
28. Aminoff D: Methods for the quantitative estimation of N-acetylneuraminic acid and their application to hydrolysate of sialomucoides. Biochem J 1961, 81:384–392
29. Neskovic N, Sarlieve L, Nussbaum JL, Kostic D, Mandel P: Quantitative thin layer chromatography of glycolipids in animal tissues. Clin Chem Acta 1972, 38:147–153
30. Ledeen RW, Yu RK: Gangliosides: structure, isolation and analysis. Methods Enzymol 1982, 83:139–192
31. Yamamoto M, Boyer AM, Schwarting GA: Fucose-containing glycolipids are stage- and region-specific antigens in developing embryonic brains of rodents. Proc Natl Acad Sci USA 1985, 82:3045–3049
32. Dahl DL, Warren CD, Rathke EJS, Jones MZ: β-Mannosidosis: prenatal detection of caprine allantoic fluid oligosaccharides with thin layer, gel permeation and high performance liquid chromatography. J Inherited Metab Dis 1986, 9:93–98
33. Warren CD, Bugge B, Linsley K, Daniels D, Daniel PF, James LF, Jeanloz RW: Locoweed toxicosis in sheep: Oligosaccharides accumulated in fetal and maternal tissues. Swainsonine and Related Glycosidase Inhibitors. Edited by LF James, AD Elbein, RJ Molyneux, CD Warren. Ames, Iowa, University Iowa Press, 1989, pp 344–359
34. Warner TG, O'Brien JS: Structure analysis of the major oligosaccharides accumulating in canine G_{M1} gangliosidosis liver. J Biol Chem 1982, 257:224–232
35. Warren CD, Alroy J, Bugge B, Daniel PF, Raghavan SS, Kolodny EH, Lamar JJ, Jeanloz RW: Oligosaccharides from placenta: early diagnosis of feline mannosidosis. FEBS Lett 1985, 195:247–252
36. Bjorkman N: Placentation. Textbook of Veterinary Histology.

Edited by HD Dellmann, EM Brown. Philadelphia, Lea & Febiger, 1976, pp 351–369

37. Lee RE: The fine structure of cerebroside occurring in Gaucher's disease. Proc Natl Acad Sci USA 1969, 61:484–489
38. Yunis EJ, Lee RE: The ultrastructure of globoid (Krabbe) leukodystrophy. Lab Invest 1969, 21:415–419
39. Kleinschmidt T, Christomanou H, Braunitaer G: Complete amino acid sequence and carbohydrate content of naturally occuring glucosylceramide activator protein (A1 activator) absent from new human Gaucher disease variant. Biol Chem Hoppe Seyler 1987, 368:1571–1578
40. Li SC, Kihara H, Serizawa S, Li YT, Fluharty AL, Mayes JS, Shapiro LJ: Activator protein required for the enzymatic hydrolysis of cerebroside sulfate deficiency in urine of patients affected with cerebroside sulfatase activator deficiency and identity with activators for enzymatic hydrolysis of G_{M1} ganglioside and glabotriaosylceramide. J Biol Chem 1985, 260:1867–1871
41. Sandhoff K, Conzelmann E, Neufeld EFG, Kaback MM, Suzuki K: The G_{M2} gangliosidoses. The Metabolic Basis of Inherited Disease, 6th Edition. Edited by Scriver CR, Beaudet AL, Sly WS, Valle D. New York, McGraw-Hill, 1989, pp 1807–1838
42. Yu RK, Saito M: Structure and localization of gangliosides. Neurobiology of Glycoconjugates. Edited by Margolis RU, Margolis RK. New York, Raven Press, 1989, pp 1–42
43. Castagnaro M, Alroy J, Ucci AA, Glew RH: Lectin histochemistry and ultrastructure of feline kidney from six different storage diseases. Virchows Arch B 1987, 54:16–26
44. Jolly RD, Slack PM, Winter PJ, Murphy CE: Mannosidosis: patterns of storage and urinary excretion of oligosaccharides in the bovine model. Aust J Exp Biol Med Sci 1980, 58:421–428
45. Lott IT, Daniel PI: Serum and urinary trisaccharides in mannosidosis. Neurology 1981, 31:1159–1162
46. Berra B, DeGasperi R, Rapelli S, Okada S, Li S-C, Li Y-T: Presence of glycoprotein containing the polylactosamine structure in brain and liver of G_{M1}-gangliosidosis patients. Comparative study between clinical types I and II, using endo-β-galactosidase enzyme. Neurochem Pathol 1986, 4:107–117
47. Williams MA, Gross SK, Evans JE, McCluer RH: Glycolipid stage-specific embryonic antigens (SSEA-1) in kidneys of male and female C57BL/6J and beige adult mice. J Lipid Res 1988, 29:1613–1619